FACTA UNIVERSITATIS (NIŠ)
SER.: ELEC. ENERG. vol. 24, no. 2, August 2011, 209-219

Numerical Modeling of DC Busbar Contacts

Dedicated to Professor Slavoljub Aleksić on the occasion of his 60th birthday

Ioan Popa and Alin-Iulian Dolan

Abstract: The paper presents two electro-thermal numerical models which can be used for the modeling and optimization of high currents busbar contacts for DC. The models are obtained by coupling of the electric model with the thermal field problem. The coupling is carried out by the source term of the differential equation which describes the thermal field. The models allows the calculation of the space distribution of the electric quantities (electric potential, the gradient of potential and the current density) and of the thermal quantities (the temperature, the temperature gradient, the Joule losses and heat flow). A heating larger than that of the busbar appears in the contact zone, caused by the contact resistance. The additional heating, caused by the contact resistance is simulated by an additional source injected on the surface of contact. The 2D model has been solved by the finite volumes method while the 3D model, by the finite elements method. Both models were experimentally validated. Using the models, one can determine the optimal geometry of dismountable contact for an imposed limit value of the temperature.

Keywords: Numerical modeling; Coupled problems; 3D Finite elements; 2D Finite Volumes; Busbar contacts.

1 Introduction

THE OPTIMIZATION of the busbar contacts (Figure 1) for high currents (1000 - 4000 A), used in the design of electrical equipment in metal envelope, is possible by solving a coupled electrical and thermal problem. The dismountable contact of a system of busbars has a non-uniform distribution of current density on the cross-section of the current leads in the contact region. The non-uniform

Manuscript received on Jun 17, 2011.

The authors are with University of Craiova, Electrical Apparatus and Technologies Department, 107 Decebal str., Craiova 200440, Romania (e-mails: [ipopa, adolan]@elth.ucv.ro).

distribution of the current density implies a non-uniform distribution of source term in the thermal conduction equation.

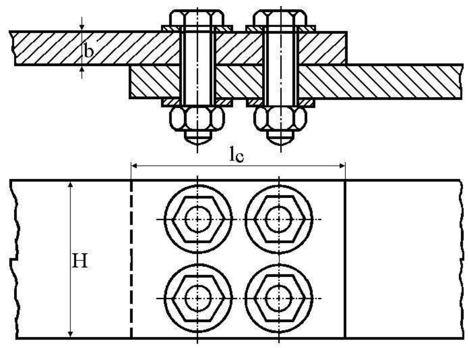

Fig. 1. Typical Busbar Contact.

The distribution of the electric quantities can be obtained by solving of Laplace equation for electric potential. The solution of this equation depends on the temperature through electric conductivity. In its turn the electric conductivity influences the source term in the thermal conduction equation and thus the value and the distribution of the temperature of contact region.

It is possible to obtain the correct distributions for the electric quantities (potential, intensity of the electric field, current density and losses by Joule effect) and thermal quantities (temperature, gradient of temperature, density of the heat flow, convection flow on the contact surface etc.) by coupling of the two problems, electric and thermal. The numerical model allows the calculation of the constriction resistance (caused by the variation of the cross section of the current leads).

2 Numerical Model

The mathematical model used for obtaining the 2D numerical model has two components, the electrical model and the thermal model, coupled by the electric conductivity, which varies according to the temperature, and the source term.

2.1 Electrical model

The electrical model is governed by a 2D model described by the Laplace equation for electric potential:

$$\frac{\partial}{\partial x}\left(\sigma(T)\frac{\partial V}{\partial x}\right)+\frac{\partial}{\partial y}\left(\sigma(T)\frac{\partial V}{\partial y}\right)=0 \tag{1}$$

where electric conductivity, and thus the electrical resistance, vary according to the temperature as:

$$\rho(T) = \rho_{20}(1+\alpha_R(T-20)) \tag{2}$$

Knowing the electric potential, one can obtain the intensity of the electric field $\vec{E} = -\mathrm{grad}V$ and the current density from law of electric conduction $\vec{J} = \sigma\vec{E}$.

The Joule losses (by the unit of volume) which represents the source term in the thermal conduction equation are calculated by the following relation:

$$S(T) = \vec{J}\cdot\vec{E} = \rho(T)J^2 = \sigma(T)E^2. \tag{3}$$

2.2 Thermal Model

The thermal model is governed by the thermal conduction equation in steady state:

$$\frac{\partial}{\partial x}\left(\lambda(T)\frac{\partial T}{\partial x}\right) + \frac{\partial}{\partial y}\left(\lambda(T)\frac{\partial T}{\partial y}\right) + S = 0 \tag{4}$$

where λ - the thermal conductivity which is considered constant in the temperature range of the current leads (bellow 200°).

3 Domain of Analysis And Boundary Conditions

One considers a simplified analysis domain which is presented in Figure 2 and Figure 3 where one neglects the existence of the fastening bolts.

The boundary conditions of the electrical model are presented in Figure 2. In the general case, one knows the current I carrying the current lead which determines a voltage drop $V_1 - V_2$. In this model, one initializes the voltage drop for which one calculates the current which corresponds to it (at each iteration) and then in another iteration loop one modifies the voltage drop to obtain the desired value of the current.

The current which passes by the section of the current lead is calculated by the following relation:

$$I = \int_S (\vec{J}\cdot\vec{n})\mathrm{d}S \tag{5}$$

where $\vec{n}$ - the normal at S which is the cross-section of the current lead.

The two assembled bars are considered sufficiently long to set, on the boundaries AB and AC, (Figure 3) the boundary conditions of Neumann homogeneous type. Because the length of segments AE and FD (375 mm) of Figure 3 is long enough the temperature distribution is uniform and consequently the temperature gradient is almost zero and the axial thermal flow is also zero.

On the other borders, one sets boundary conditions of the convection type, with a global heat exchange coefficient h (by convection and radiation, $h = 14.5$ $\mathrm{Wm^{-2}K^{-1}}$, increased by a coefficient that takes into acount the heat transfer through the side surfaces) to the environment having the temperature T_∞ [1].

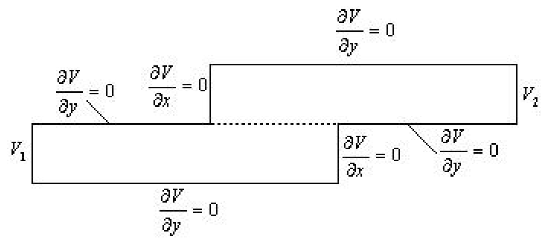

Fig. 2. Analysis Domain and Boundary Conditions for Electrical Model.

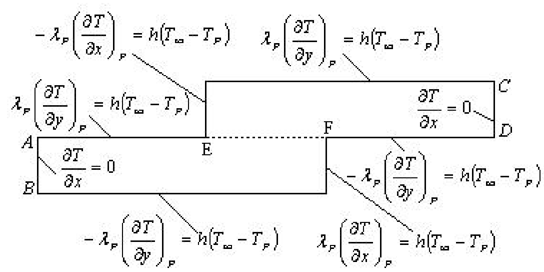

Fig. 3. Analysis Domain and Boundary Conditions for Thermal Model ($AE = FD = 0.375$ m, $EF = 0.1$ m).

4 Numerical Algorithm

The numerical model is obtained by the discretization of the differential equations (1) and (4) using the finite volumes method [2]. The coupled model is of alternate type [3] where the equations are solved separately and coupling is realized by the transfer of the data of one problem to the other. The two problems (electric and thermal) are integrated in the same source code and thus use the same mesh. The numerical algorithm is shown in Figure 4. The criterion of convergence of the coupled model was selected the value of the current, through the current lead, calculated using the relation (5). One used a mesh having 3787 nodes (with $\Delta x = \Delta y = 1.66$ mm). The imposed percent relative error, for electrical and thermal models, was 10^{-7} and for coupled model was 10^{-5}. The convergence of the coupled model is very fast ($4 \div 6$ iterations). If the error is reduced then the number of iterations increases but this is not necessary. The desired value of the current in contact is adjusted by varying the voltage drop on contact. The number of iterations for the electrical and thermal models decreases sharply with the stabilization of current.

The numerical validation of the model was made using a simplified analysis domain with a current lead with variable cross-section [1,4]. The numerical validation of the results of this simplified model was made by using the software QuickField Professional for the electrical and thermal models. There is a very good agreement between our results and the results obtained using the QuickField software.

5 Numerical Results and Experimental Validation

The Figures 5, 6, 7, 8 and 9 present some numerical results. The dimensions of the analysis domain are those of Figure 3. The principal difficulty, in modelling the temperature distribution of a dismountable contact, is to take into account the resistance of contact (especially disturbance resistance). The contact resistance model is presented in the next paragraph. The optimization of the contact design means calculation of the dimension l_c such that the maximum temperature, in the contact region, remains lower than the acceptable limiting value allowed by standards.

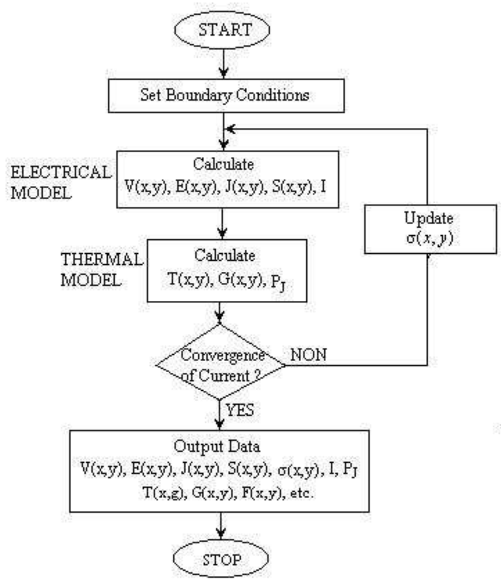

Fig. 4. Simplified Diagram of Numerical Algorithm.

For the case presented ($l_c = 100$ mm and $I = 620$ A) the calculated losses by Joule effect with constriction resistance are 28.89 W, while calculated Joule losses without constriction resistance are 24.91 W. Varying overlapping length of the bars l_c (see Figure 1) the maximum contact temperature has a linear dependence with l_c [1].

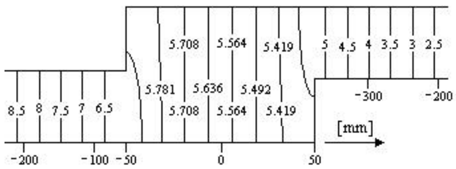

Fig. 5. Potential Distribution in the Contact Region (in mV).

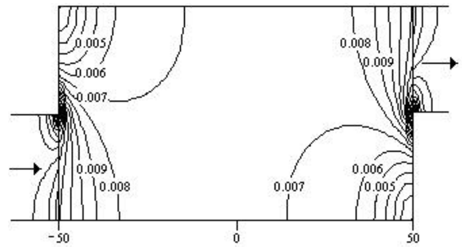

Fig. 6. Electrical Field Distribution in the Contact Region (in V/m).

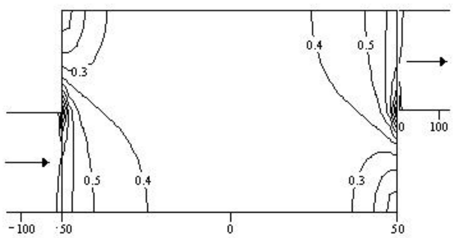

Fig. 7. Current Density Distribution in the Contact Region (in A/mm^2).

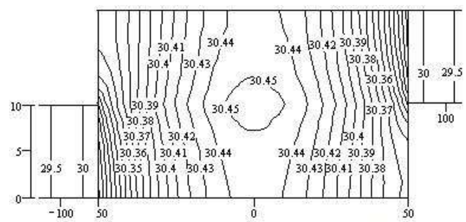

Fig. 8. Temperature Distribution in the Contact Region (in °C).

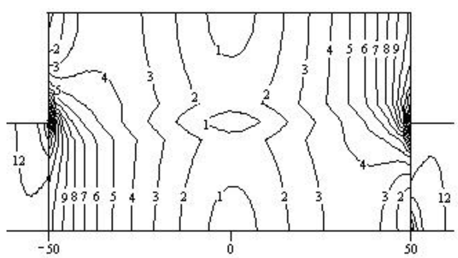

Fig. 9. Gradient of Temperature in the Contact Region (in °C).

6 3D Numerical Model

The 3D model was obtained using the software Flux 3D by coupling the AC Magnetics problem at zero frequency with the transient thermal problem [5]. The mesh were realised using first order tetrahedral elements (Figure 10). The injected current in busbar was modeled by a current source connected to a solid conductor using the module Electric Flux (Figure 11).

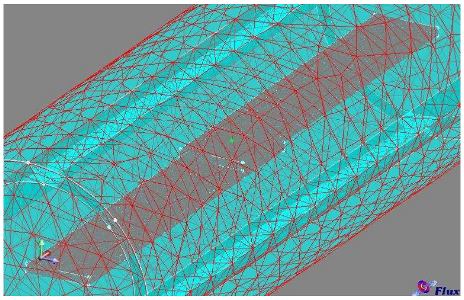

Fig. 10. 3D Mesh (269137 elements).

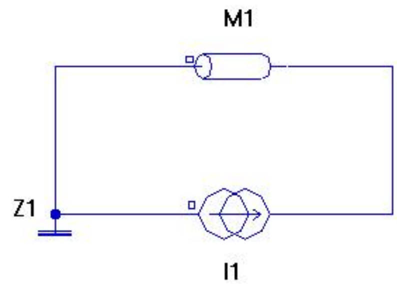

Fig. 11. Electric circuit of busbar contact.

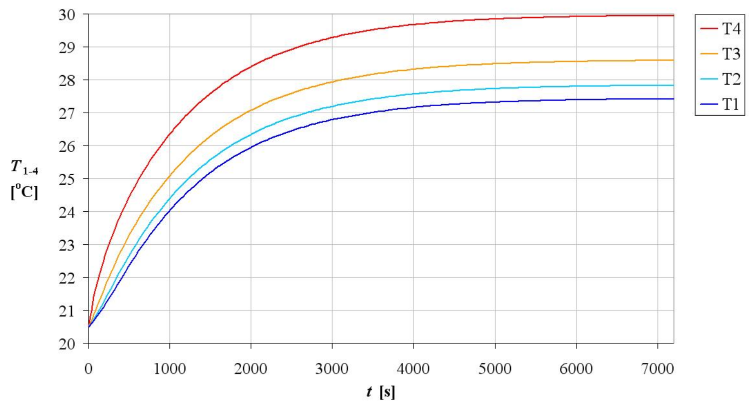

Fig. 12. Time evolution of temperature in fixed points.

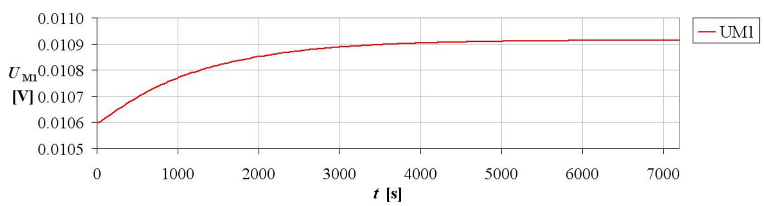

Fig. 13. Time evolution of voltage drop on busbar contact.

The numerical 3D results are shown in Figures 12 - 15 and the spatial distributions of magnetic flux density and thermal field in steady state in Figures 16 and 17.

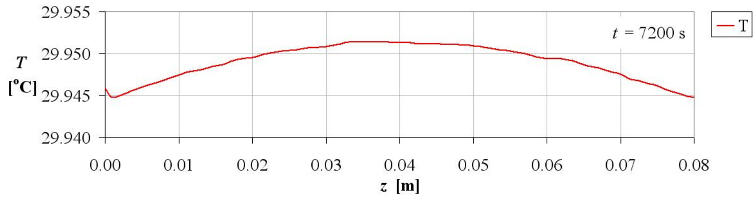

Fig. 14. Temperature distribution on cross section in steady state.

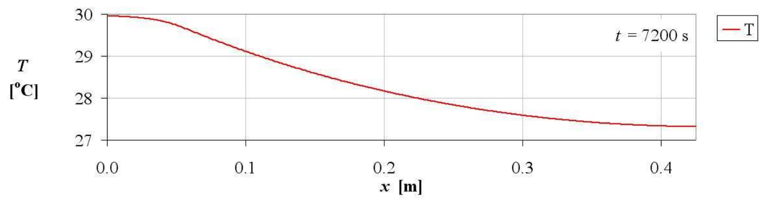

Fig. 15. Temperature distribution along of busbar in steady state.

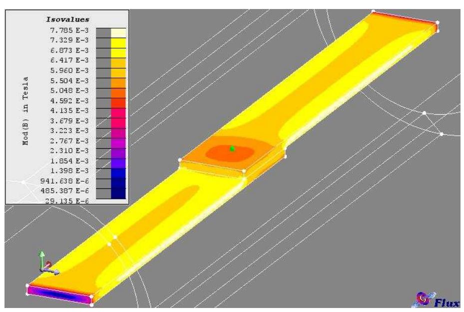

Fig. 16. Magnetic flux density distribution on busbar.

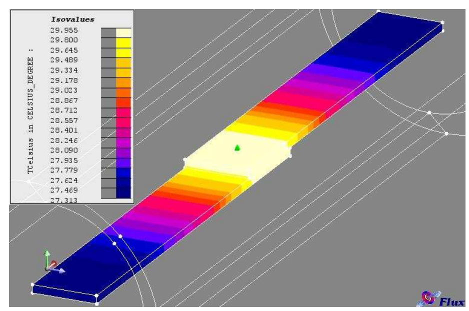

Fig. 17. Temperature distribution on busbar in steady state.

For the validation of the numerical model an experimental model was built with the measuring points presented in Figure 18 (the measuring points are placed in the center of surface). The values measured in these points, using a digital thermometer with contact (Fluke 54 II) are shown in Table 1.

Table 1. : Experimental Results

Point	T_1	T_2	T_3	T_4	T_5	T_6	T_7
T[°C]	29.3	29.3	29.4	29.8	29.4	29.3	29.3

The 2D numerical results for the thermal field, ilustrated in Figure 8, compared with the experimental results (see Table 1) show a good agreement. For exemple the error in the measurement point T4 (in the center of the contact) for 2D model is 2.13 % and for 3D model is 0.51 %. The experimental data of Table 1 were measured for a tightening force of screws of 100 N.

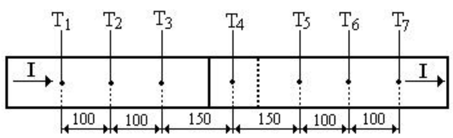

Fig. 18. Points of Temperature Measurement.

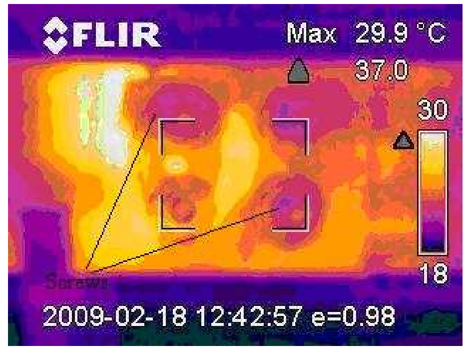

Fig. 19. Thermal Image of the Contact Region.

For the considered contact geometry and the current of $I = 620$ A, the voltage drop measured between the limits *AB* and *AC* (see Figure 4) was 11.98 mW, while the voltage drop controled to get the current imposed in the numerical model 2D was 11.2 mV . The experimental results of Table 1 were obtained for the ambient temperature of 20.5 °C.

Figure 19 shows the thermal image of the contact zone obtained with the thermal camera. One can observe the scews areas which is colder. The scews help to cool the contact region by enlarging the surface of thermal eschange with surrouding environment.

7 Contact Resistance Model

The source term determined by the contact resistance is calculated by the following relation:

$$S_c = \frac{R_c I^2}{(n_c - 1)\Delta x \Delta y H} \tag{6}$$

where Δx and Δy - the dimensions of the control volume, n_c - the number of mesh points in the contact region (see Figure 20), H - the bus bar width (see Figure 1).

The contact resistance $R)c$ is calculated with the following relation [6]:

$$R_c = \frac{\rho}{\pi a n} \arctan \frac{\sqrt{d^2 - a^2}}{a} - 1.2 \frac{\rho \sqrt{d^2 - a^2}}{A_a} + \frac{R_{ss}}{n \pi a^2} \tag{7}$$

where ρ - the electric resistivity, n - the number of contact points, A_a - the total area of contact (see Figure 14) and R_{ss} - the specific resistance of oxide film of contact point (in Ωm^2).

The radius of contact surface a is calculated from Holm's relation:

$$a = \sqrt{\frac{F}{\pi n \xi H_d}} \tag{8}$$

where F - the tightening force, ξ - Prandtl coefficient, H - material durity.

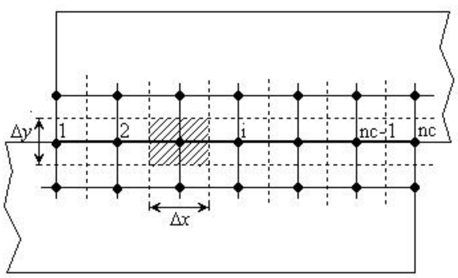

Fig. 20. The Mesh in Contact Region.

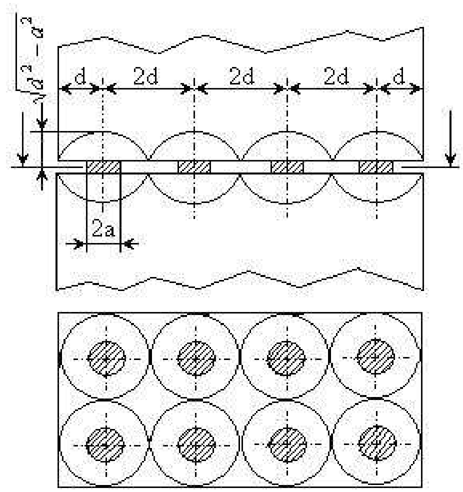

Fig. 21. Physical Model of Contact Region.

The relation (7) does not take into account the variation of contact resistance with temperature. To take it into account one can use the relation [6]:

$$R_c(T) = R_c(20)\left(1 + \frac{2}{3}\alpha_R(T - 20)\right) \tag{9}$$

where α_R - the variation coefficient of electric resistivity with temperature, $R_c(20)$ - the contact resistance at 20°C. The contact resistance model was implemented in numerical model of dismountable contact. For a constant value of the current ($I = 620$ A), varying the tightening force of the screws one can get the variation of the maximum temperature versus tightening force.

8 Conclusions

The presented model can be used for the optimization of the current leads of high currents with variable cross-section, such as the dismountable contacts of busbar. The model allows the calculation of the constriction resistance of current lead, the constriction resistance of contact region and takes into account the specific resistance of oxide film of contact point which is an important component of the contact resistance.

Numerical model created allows evaluation of the maximum temperature in the contact area as a function of the tightening force of the dismountable contact.

An improvement of the model is possible taking into account the presence of the tightening screws and usage of the model of contact resistance moore precise as example the model given by Greenwood [7, 8]. The model is valid only for dc. In alternating current Equation (1) must be replaced by a magneto-dynamic equation.

Acknowledgements

The authors wish to thank the CEDRAT Groupe (France) kindly enough to make available for a month and half a software license of FLUX through which we obtained the 3D results presented in this paper.

References

[1] I. Popa, I. aand Cautil and D. Floricau, "Modeling and optimization of high currents dismountable contacts," *WSEAS Transaction on Power Systems*, vol. 1, no. 9, pp. 1641 – 1646, 2006.

[2] I. Popa, *Modélisation numérique du transfert thermique. Méthode des volumes finis*. Universitaria, Craiova, 2002.

[3] G. Meunier, *Electromagnétisme et problémes couplés*, Paris, 2002.

[4] I. Popa, I. Cautil, and D. Floricau, "Modéle numérique électrothermique pour l'optimisation des contacts démontables de forts courants," *Annals of the University of Craiova - Electrical Engineering Series*, vol. 30, no. 30, pp. 330 – 333, 2006.

[5] "Flux 10.3, guide d'utilisation," 2009, volume 3, Les applications physiques.

[6] G. Hortopan, *Aparate electrice de comutaçie*. Tehnică, Bucureşti, 1993, (in Romanian).

[7] S. Schofy, J. Kindersberger, and H. Lobl, "Joint resistance of busbar-joints with randomly rouggh surfaces," in *Proc. of 21th Conference on Electrical Contacts*, Zurich, 2002, pp. 230 – 237.

[8] Z. Feng, S. S. Babu, M. L. Santella, B. W. Riemer, and J. E. Gould, "An incrementally coupled electrical-thermal-mechanical model for resistance spot welding," in *Proceedings of 5th International Conference on Trends in Welding Research*, Pine Mountain, GA, 1998, pp. 1–6.